A Continuum Schwinger Function Method for Baryon Spectra and Structure

Jorge Segovia

INP at Nanjing University, and
University Pablo de Olavide, in Seville

Revealing Emergent Mass Through Studies of Hadron Spectra and Structure

ECT* Workshop, Italy, September 12-16, 2022

Emergence

Low-level rules producing high-level phenomena with enormous apparent complexity

Start from the QCD Lagrangian:

$$\mathcal{L}_{\rm QCD} = \bar{\psi}(i\not{D} - m)\psi - \frac{1}{4} G_a^{\mu\nu} G^a_{\mu\nu} + \frac{1}{2\xi}(\partial^\mu A^a_\mu)^2 + \partial^\mu \bar{c}^a \partial_\mu c^a + g\, f^{abc}(\partial^\mu \bar{c}^a) A^b_\mu c^c \,.$$

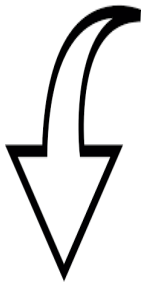

Lattice-regularized QCD, Continuum Schwinger-function methods, ...

And obtain:

- Dynamical generation of fundamental mass scale in pure Yang-Mills (gluon mass).
- Quark constituent masses and dynamical chiral symmetry breaking.
- Bound state formation: mesons, baryons, glueballs, hybrids, multiquark systems...
- Signals of confinement.

These (emergent) phenomena is not apparent in the QCD Lagrangian; however, they characterized the nonperturbative regime of QCD where hadrons live

Emergent phenomena *could be associated with dramatic, dynamically driven changes in the analytic structure of QCD's Schwinger functions, which are solutions of the DSEs*

Quark propagator:

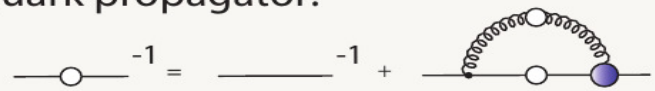

Ghost propagator:

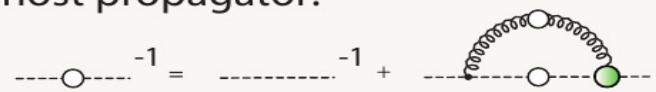

Ghost-gluon vertex:

Gluon propagator:

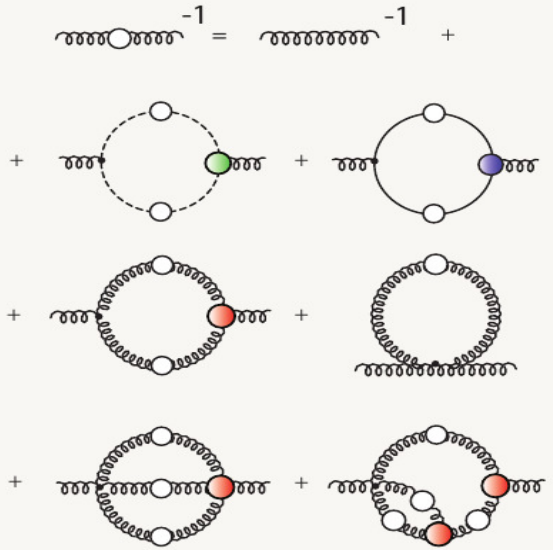

Quark-gluon vertex:

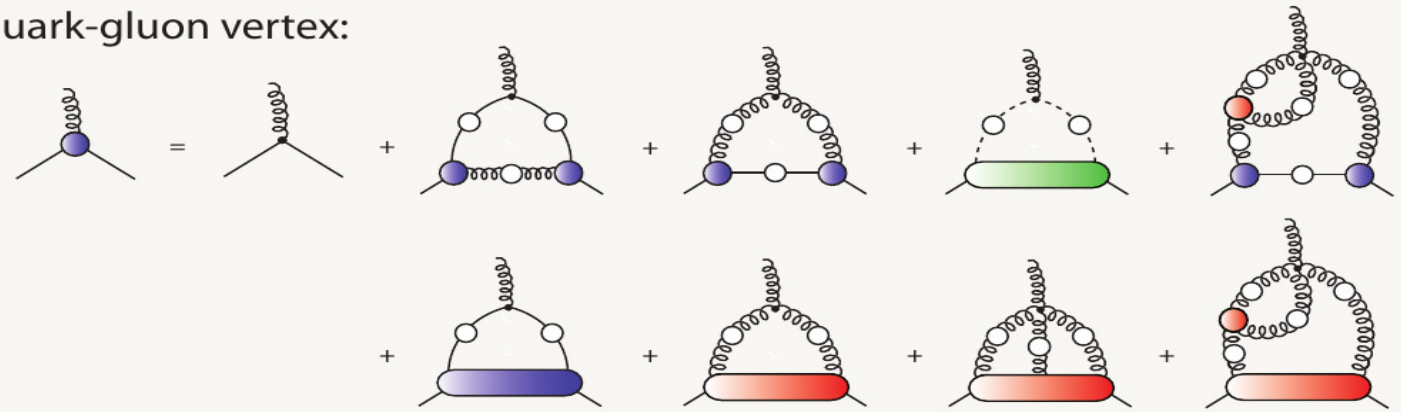

Off-shell Green's (correlation) functions

☞ Even though they are:

- Gauge dependent.
- Renormalization point and scheme dependent.

☞ However:

- They capture characteristic features of the underlying dynamics, both perturbative and non-perturbative.
- When appropriately combined they give rise to physical observables.

Theory tool based on Dyson-Schwinger equations

☞ Interesting features:

- Inherently non-perturbative but, at the same time, captures the perturbative behavior $\rightarrow$ accommodates the full range of physical momenta.
- Cover smoothly the full quark mass range, from the chiral limit to the heavy-quark domain.

☞ Main caveats:

- Truncation of the infinite system of coupled non-linear integral equations that preserves the underlying symmetries of the theory.
- No expansion parameter $\rightarrow$ no formal way of estimating the size of the omitted terms $\leftrightarrow$ the projection of higher Green's functions on the lower ones is small.

Non-perturbative QCD: Dynamical generation of gluon mass

☞ Dressed-gluon propagator in Landau gauge:

$$i\Delta_{\mu\nu} = -iP_{\mu\nu}\Delta(q^2), \quad P_{\mu\nu} = g_{\mu\nu} - q_\mu q_\nu / q^2$$

- An inflexion point at $q^2 > 0$.
- Breaks the axiom of reflexion positivity.
- Gluon mass generation $\leftrightarrow$ Schwinger mechanism.

A.C. Aguilar *et al.*, Phys. Rev. D78 (2008) 025010;
I.L. Bogolubsky *et al.*, Phys. Lett. B676 (2009) 69.

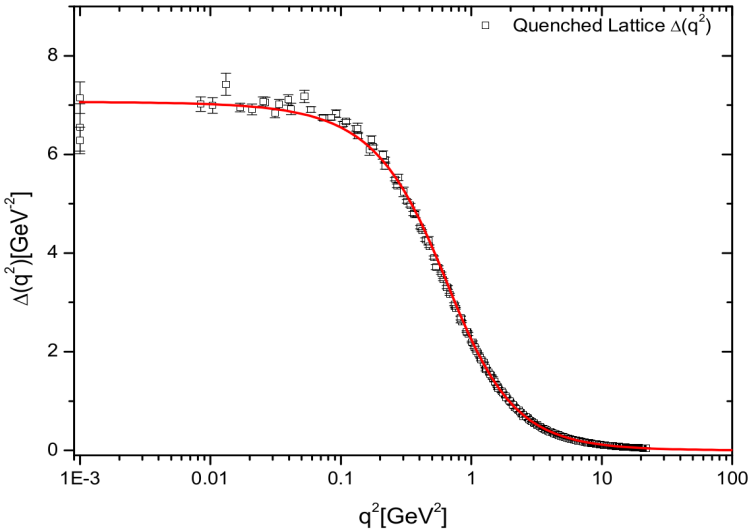

☞ Dressed-ghost propagator in Landau gauge:

$$G^{ab}(q^2) = \delta^{ab}\,\frac{J(q^2)}{q^2}$$

- No power-like singular behavior at $q^2 \to 0$.
- Good indication that $J(q^2)$ reaches a plateau.
- Saturation of ghost's dressing function.

Ph. Boucaud *et al.*, JHEP 0806 (2008) 099;
C. Fischer *et al.*, Annals Phys. 324 (2009) 2408.

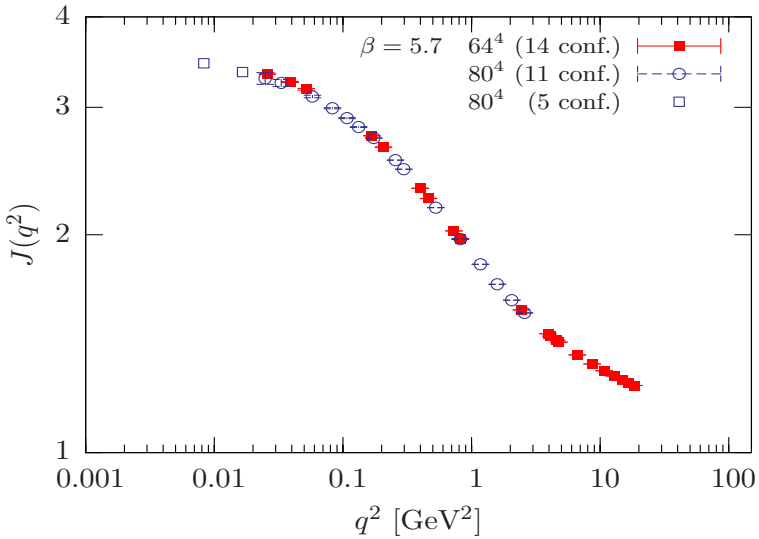

Non-perturbative QCD: Saturation at IR of process-independent effective-charge

D. Binosi *et al.*, Phys. Rev. D96 (2017) 054026;
A. Deur *et al.*, Prog. Part. Nucl. Phys. 90 (2016) 1-74.

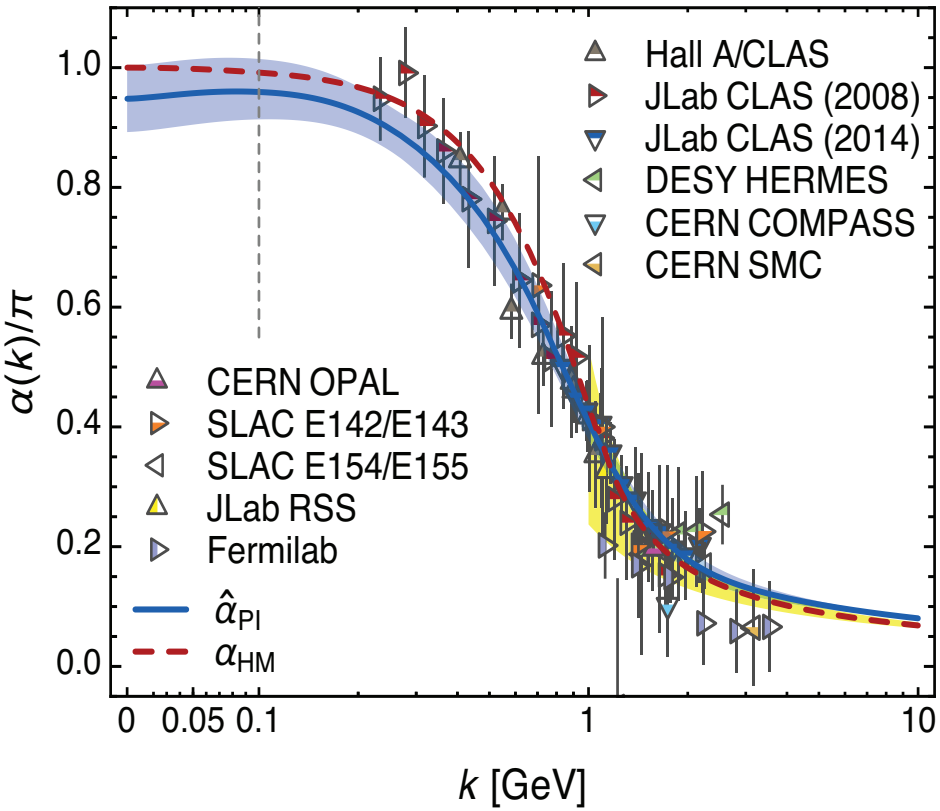

- Data = running coupling defined from the Bjorken sum-rule.

$$\int_0^1 dx \left[g_1^p(x,k^2) - g_1^n(x,k^2) \right] = \frac{g_A}{6} \left[1 - \frac{1}{\pi} \alpha_{g_1}(k^2) \right]$$

- Curve determined from combined continuum and lattice analysis of QCD's gauge sector (massless ghost and massive gluon).
- The curve is a running coupling that does NOT depend on the choice of observable.
  - No parameters.
  - No matching condition.
  - No extrapolation.
- It predicts and unifies an enormous body of empirical data via the matter-sector bound-state equations.

- Perturbative regime:

$$\alpha_{g_1}(k^2) = \alpha_{\overline{\rm MS}}(k^2) \left[1 + 1.14 \alpha_{\overline{\rm MS}}(k^2) + \dots \right]$$

$$\hat{\alpha}_{\rm PI}(k^2) = \alpha_{\overline{\rm MS}}(k^2) \left[1 + 1.09 \alpha_{\overline{\rm MS}}(k^2) + \dots \right]$$

Non-perturbative QCD: Dynamical generation of quark mass

☞ Dressed-quark propagator in Landau gauge:

$$S^{-1}(p) = Z_2(i\gamma\cdot p + m) + \Sigma(p) = \left(\frac{Z(p^2)}{i\gamma\cdot p + M(p^2)}\right)^{-1}$$

- Mass generated from the interaction of quarks with the gluon-medium.
- Light quarks acquire a HUGE constituent mass.
- Responsible of the 98% of proton's mass, the large splitting between parity partners, . . .

M.S. Bhagwat *et al.*, Phys.Rev. C68 (2003) 015203.

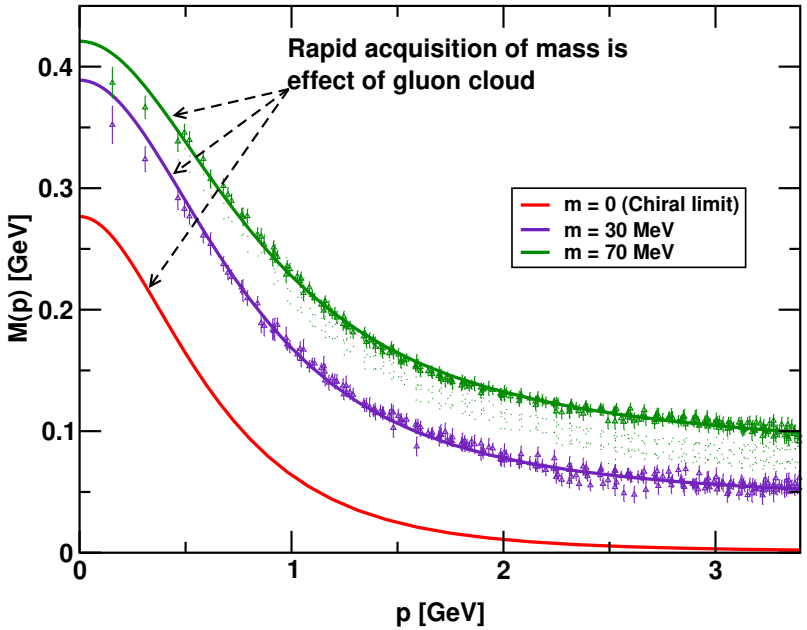

☞ Goldberger-Treiman relation at the quark level:

Quark propagator: $S^{-1}(p) = i\gamma\cdot p\, A(p^2) + B(p^2)\,,$

Pion's BS-amplitude: $\Gamma_\pi(p,P) \propto \gamma^5 E_\pi(p;P)\,.$

$$f_\pi E_\pi(p;0) = B(p^2)$$

Properties of the massless pion are a direct measure of the dressed-quark mass function

Cleanest expression of the mechanism that is responsible for almost all the visible mass in the universe

Diquark correlations

Any interaction able to create Goldstone modes as bound-states of light dressed-quark and -antiquark will generate strong $\bar{3}_c$ correlations between any two dressed quarks.

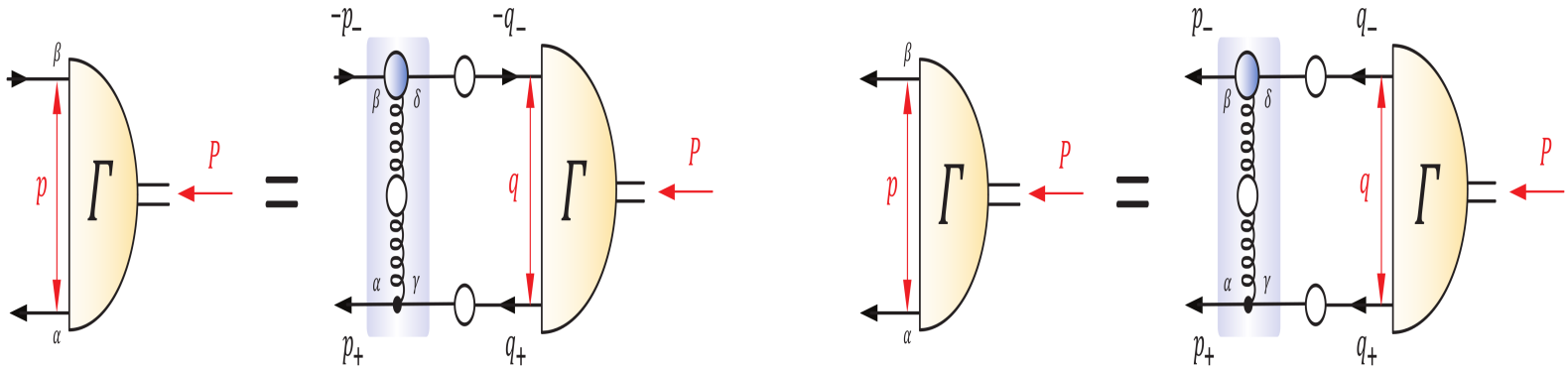

Meson BSE

Diquark BSE

☞ Owing to properties of charge-conjugation, a diquark with spin-parity J^P may be viewed as a partner to the analogous J^{-P} meson:

$$\Gamma_{q\bar{q}}(p;P) = -\int \frac{d^4q}{(2\pi)^4}\, g^2 D_{\mu\nu}(p-q)\frac{\lambda^a}{2}\gamma_\mu\, S(q+P)\Gamma_{q\bar{q}}(q;P)S(q)\,\frac{\lambda^a}{2}\,\gamma_\nu$$

$$\Gamma_{qq}(p;P)C^\dagger = -\frac{1}{2}\int \frac{d^4q}{(2\pi)^4}\, g^2 D_{\mu\nu}(p-q)\frac{\lambda^a}{2}\gamma_\mu\, S(q+P)\Gamma_{qq}(q;P)C^\dagger S(q)\,\frac{\lambda^a}{2}\,\gamma_\nu$$

☞ Whilst no pole-mass exists, the following mass-scales express the strength and range of the correlation:

$$m_{[ud]_{0^+}} = 0.7-0.8\,\text{GeV}, \quad m_{\{uu\}_{1^+}} = 0.9-1.1\,\text{GeV}, \quad m_{\{dd\}_{1^+}} = m_{\{ud\}_{1^+}} = m_{\{uu\}_{1^+}}$$

☞ Diquark correlations are soft, they possess an electromagnetic size:

$$r_{[ud]_{0^+}} \gtrsim r_\pi, \qquad r_{\{uu\}_{1^+}} \gtrsim r_\rho, \qquad r_{\{uu\}_{1^+}} > r_{[ud]_{0^+}}$$

Diquark species

Octet and decuplet baryons

	[nn]	{nn}	[ns]	{ns}	{ss}
N	●	●			
Δ		●			
Λ	●		●	●	
Σ		●	●	●	
Ξ			●	●	●
Ω					●

Other baryons as parity partners

- ☞ $[I = 0, J^P = 0^+]$: Isoscalar-scalar.
- ☞ $[I = 1, J^P = 1^+]$: Isovector-pseudovector.
- ☞ $[I = 0, J^P = 0^-]$: Isoscalar-pseudoscalar.
- ☞ $[I = 0, J^P = 1^-]$: Isoscalar-vector.
- ☞ $[I = 1, J^P = 1^-]$: Isovector-vector.

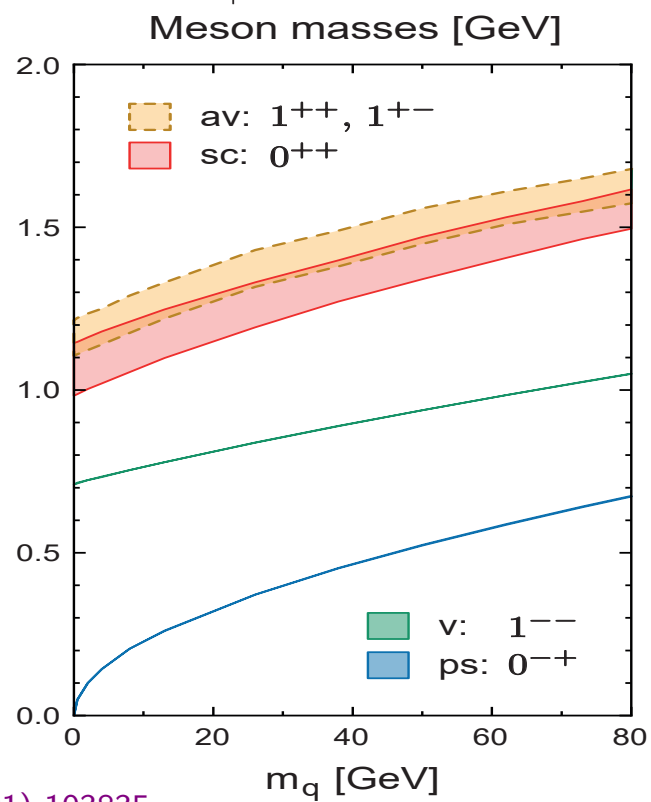

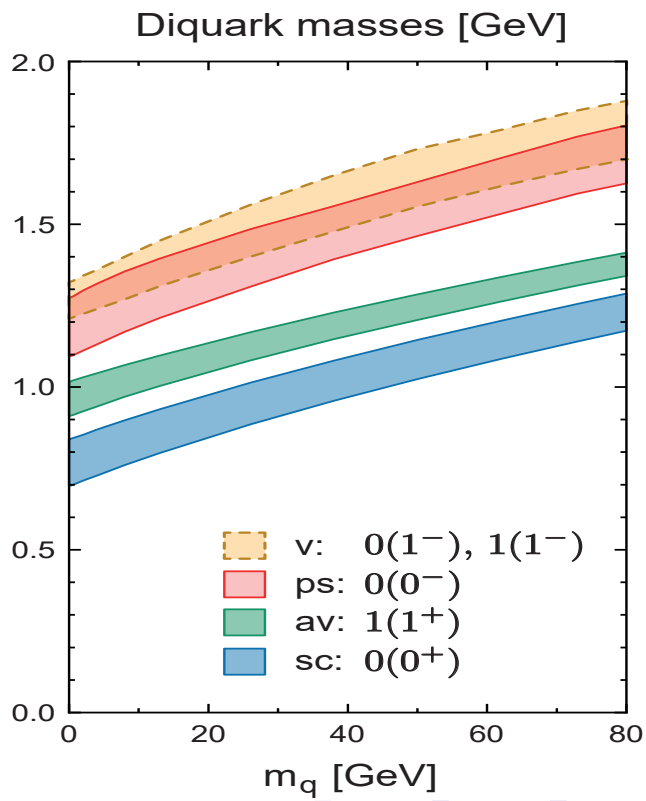

M. Yu. Barabanov *et al.*,
Prog. Part. Nucl. Phys. 116 (2021) 103835

The quark+diquark structure of a baryon

☞ A baryon can be viewed as a **Borromean bound-state**, the binding within which has two contributions:

- Formation of tight diquark correlations.
- Quark exchange depicted in the shaded area.

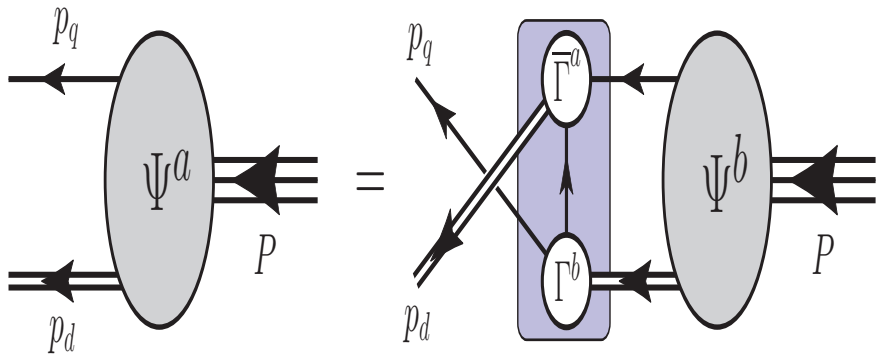

☞ The exchange ensures that diquark correlations within the baryon are fully dynamical: no quark holds a special place.

☞ The rearrangement of the quarks guarantees that the baryon's wave function complies with Pauli statistics.

☞ The number of states in the spectrum of baryons obtained is similar to that found in the three-constituent quark model, just as it is in today's LQCD calculations.

☞ Modern diquarks are different from the old static, point-like diquarks which featured in early attempts to explain the so-called missing resonance problem.

☞ Modern diquarks enforce certain distinct interaction patterns for the singly- and doubly-represented valence-quarks within the baryon.

S.-S. Xu *et al.*, Phys. Rev. D92 (2015) 114034; Y. Lu *et al.*, Phys. Rev. C96 (2017) 015208; C. Chen *et al.*, Phys. Rev. D100 (2019) 054009; P.-L. Yin *et al.*, Phys. Rev. D100 (2019) 034008.

non-relativistic | **relativistic**

Mesons: $P = (-1)^{L+1}$ ~~$P = (-1)^{L+1}$~~

S	L	J^{PC}
0	0	0^{-+}
1	0	1^{--}
0	1	1^{+-}
1	1	0^{++}

Bethe,Salpeter, Llewelyn-Smith 1950ies

$$\Gamma_\pi(P,p) = \gamma_5 \left[F_1(P,p) + F_2(P,p) i\not{P} + F_3(P,p) p P i\not{p} + F_4(P,p)[\not{p}, \not{P}]\right]$$

s-wave

p-wave

Baryons: $P = (-1)^{L}$ ~~$P = (-1)^{L}$~~

S	L	J^{P}
1/2	0	$1/2^+$
3/2	2	

J^P	total	s-wave	p-wave	d-wave	f-wave
1/2+	64	8	36	20	
3/2+	128	4	36	60	28

Masses of the octet and decuplet

- The computed masses are uniformly larger than the corresponding empirical values.
- The quark-diquark kernel omits all resonant contributions associated with meson-baryon final state interactions, which typically generate a measurable reduction.
- The Faddeev equations analyzed to produce the results should be understood as producing the dressed-quark core of the bound state, not the completely dressed and hence observable object.

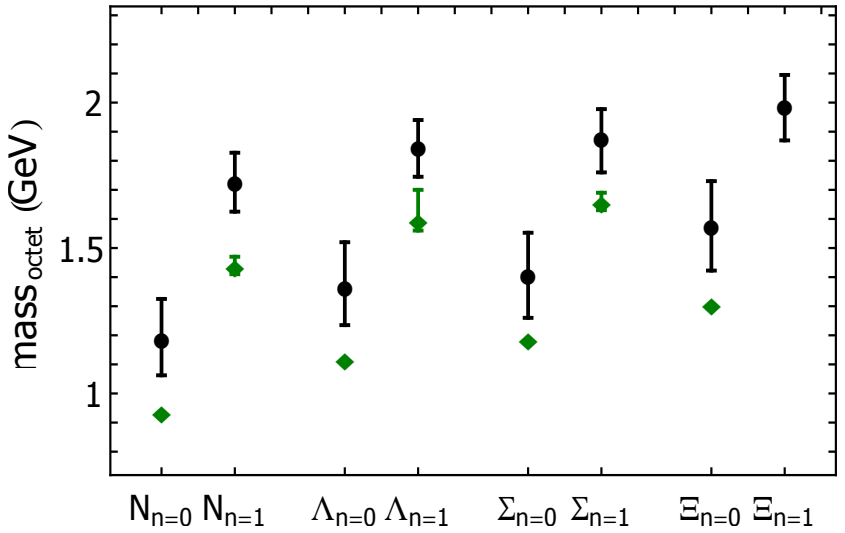

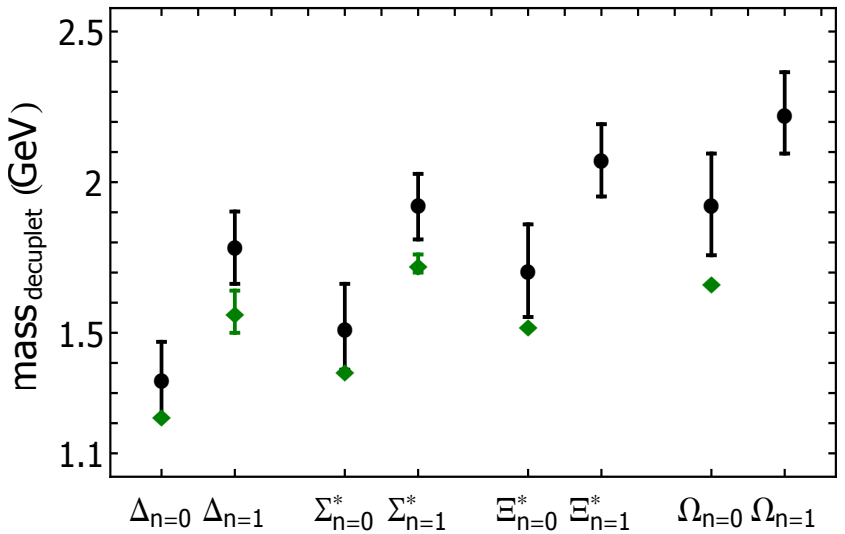

C. Chen *et al.*, Phys. Rev. D100 (2019) 054009.

Angular momenta of the octet and decuplet (I)

L content	$N_{n=0}$	$N_{n=1}$	$\Lambda_{n=0}$	$\Lambda_{n=1}$	$\Sigma_{n=0}$	$\Sigma_{n=1}$	$\Xi_{n=0}$	$\Xi_{n=1}$
S, P, D	1.19	1.73	1.37	1.85	1.41	1.88	1.58	1.99
$-, P, D$	–	–	–	–	–	–	–	–
$S, -, D$	1.24	1.71	1.40	1.83	1.42	1.84	1.59	1.97
$S, P, -$	1.20	1.74	1.37	1.85	1.41	1.89	1.58	1.99
$S, -, -$	1.24	1.71	1.40	1.83	1.42	1.84	1.59	1.97

L content	$\Delta_{n=0}$	$\Delta_{n=1}$	$\Sigma^*_{n=0}$	$\Sigma^*_{n=1}$	$\Xi^*_{n=0}$	$\Xi^*_{n=1}$	$\Omega_{n=0}$	$\Omega_{n=1}$
S, P, D, F	1.35	1.79	1.52	1.93	1.71	2.08	1.93	2.23
$-, P, D, F$	–	–	–	–	–	–	–	–
$S, -, D, F$	1.36	1.75	1.52	1.90	1.71	2.06	1.93	2.22
$S, P, -, F$	1.35	1.82	1.52	1.95	1.71	2.09	1.93	2.24
$S, P, D, -$	1.35	1.79	1.52	1.93	1.71	2.08	1.93	2.23
$S, -, -, -$	1.35	1.80	1.52	1.93	1.71	2.08	1.93	2.23

- No state is generated by the Faddeev equation unless S-wave components are contained in the wave function.
- This observation provides support in quantum field theory for the constituent quark model classification of these systems.
- The P- and D-wave components play a measurable role in, respectively, octet and decuplet baryons.

Angular momenta of the octet and decuplet (I)

L content	$N_{n=0}$	$N_{n=1}$	$\Lambda_{n=0}$	$\Lambda_{n=1}$	$\Sigma_{n=0}$	$\Sigma_{n=1}$	$\Xi_{n=0}$	$\Xi_{n=1}$
S,P,D	1.19	1.73	1.37	1.85	1.41	1.88	1.58	1.99
$-,P,D$	–	–	–	–	–	–	–	–
$S,-,D$	1.24	1.71	1.40	1.83	1.42	1.84	1.59	1.97
$S,P,-$	1.20	1.74	1.37	1.85	1.41	1.89	1.58	1.99
$S,-,-$	1.24	1.71	1.40	1.83	1.42	1.84	1.59	1.97

L content	$\Delta_{n=0}$	$\Delta_{n=1}$	$\Sigma^*_{n=0}$	$\Sigma^*_{n=1}$	$\Xi^*_{n=0}$	$\Xi^*_{n=1}$	$\Omega_{n=0}$	$\Omega_{n=1}$
S,P,D,F	1.35	1.79	1.52	1.93	1.71	2.08	1.93	2.23
$-,P,D,F$	–	–	–	–	–	–	–	–
$S,-,D,F$	1.36	1.75	1.52	1.90	1.71	2.06	1.93	2.22
$S,P,-,F$	1.35	1.82	1.52	1.95	1.71	2.09	1.93	2.24
$S,P,D,-$	1.35	1.79	1.52	1.93	1.71	2.08	1.93	2.23
$S,-,-,-$	1.35	1.80	1.52	1.93	1.71	2.08	1.93	2.23

- No state is generated by the Faddeev equation unless S-wave components are contained in the wave function.
- This observation provides support in quantum field theory for the constituent quark model classification of these systems.
- The P- and D-wave components play a measurable role in, respectively, octet and decuplet baryons.

Angular momenta of the octet and decuplet (II)

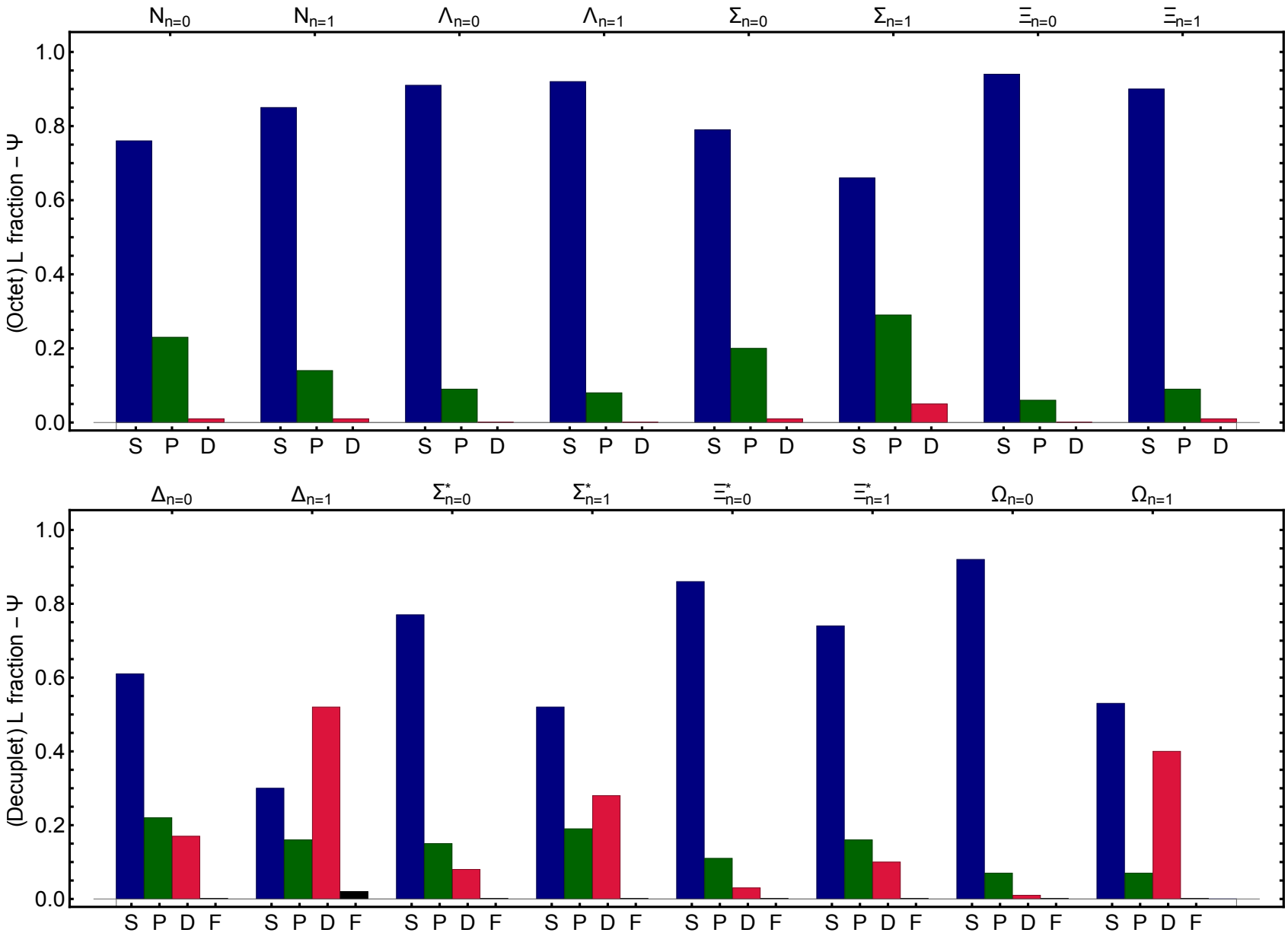

Angular momenta of the octet and decuplet (II)

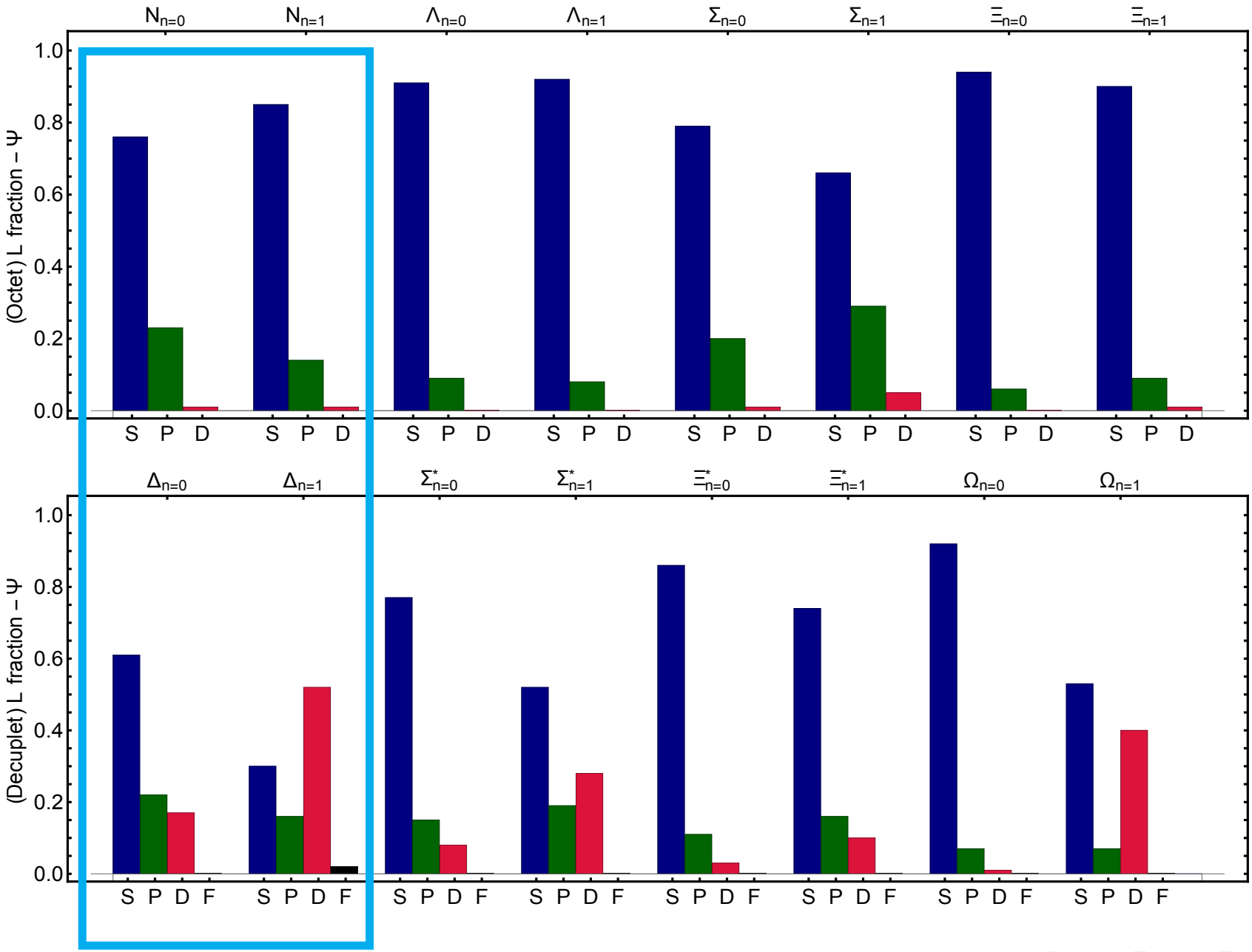

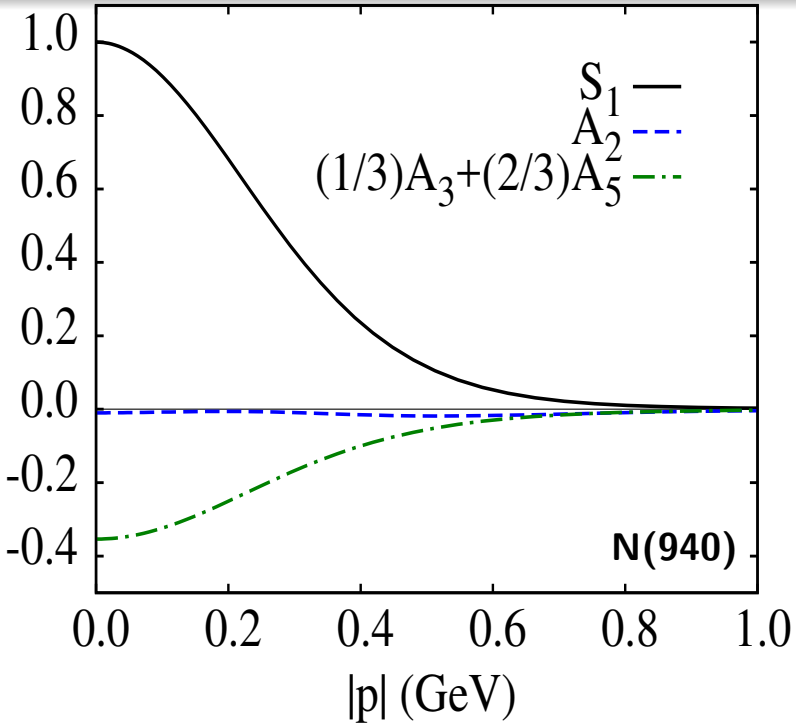
1.0
0.8
0.6
0.4
0.2
0.0
-0.2
-0.4
S1
A2
(1/3)A3+(2/3)A5
N(940)
0.0
0.2
0.4
0.6
0.8
1.0
|p| (GeV)

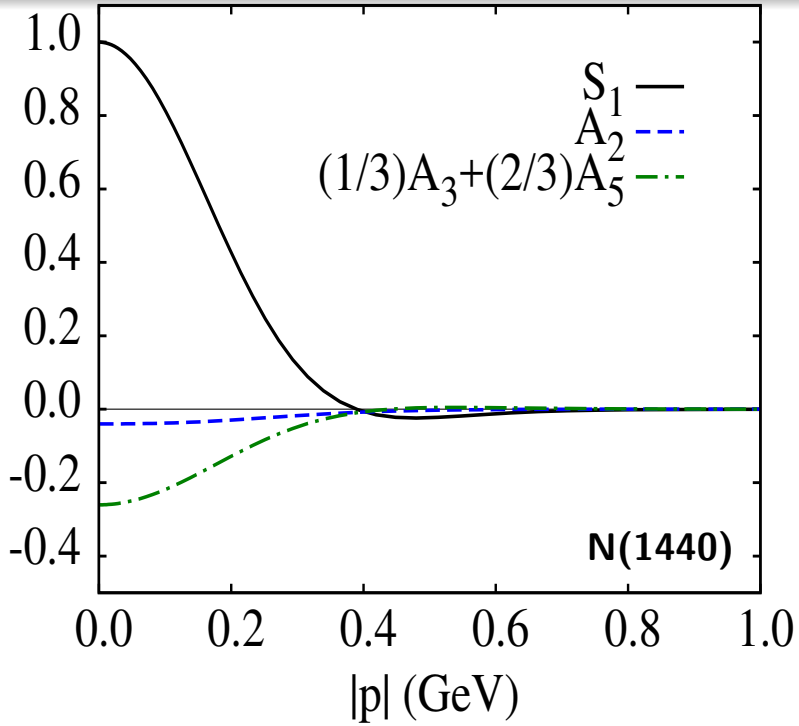
1.0
0.8
0.6
0.4
0.2
0.0
-0.2
-0.4
S1
A2
(1/3)A3+(2/3)A5
N(1440)
0.0
0.2
0.4
0.6
0.8
1.0
|p| (GeV)

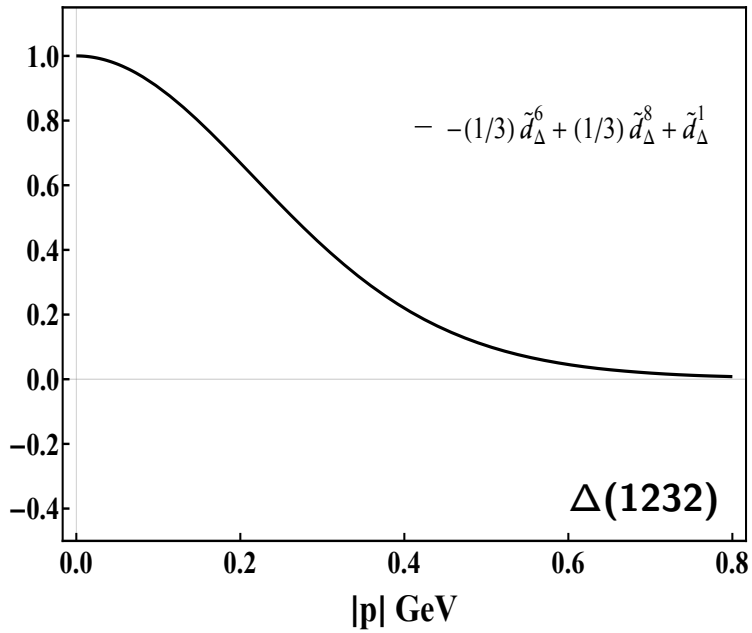
1.0
0.8
0.6
0.4
0.2
0.0
−0.2
−0.4
− −(1/3) $\tilde{d}^6_\Delta$ + (1/3) $\tilde{d}^8_\Delta$ + $\tilde{d}^1_\Delta$
Δ(1232)
0.0
0.2
0.4
0.6
0.8
|p| GeV

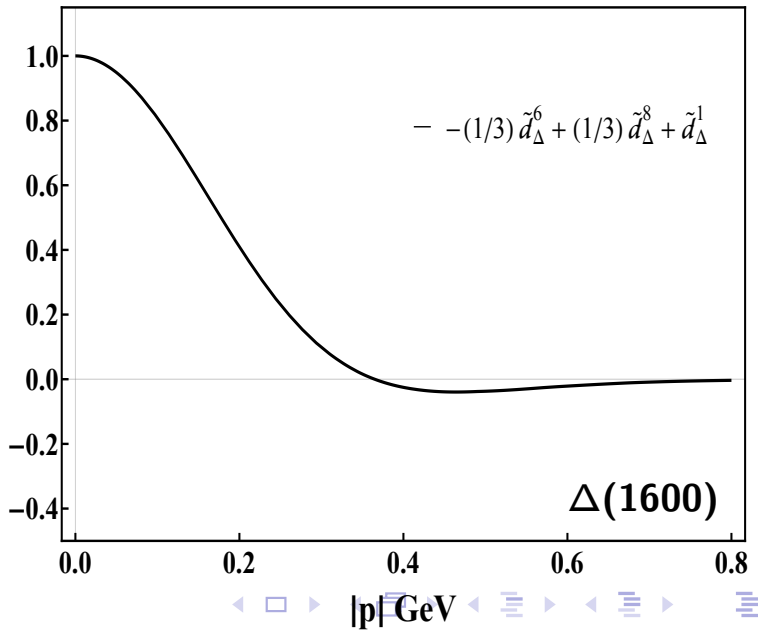
1.0
0.8
0.6
0.4
0.2
0.0
−0.2
−0.4
− −(1/3) $\tilde{d}^6_\Delta$ + (1/3) $\tilde{d}^8_\Delta$ + $\tilde{d}^1_\Delta$
Δ(1600)
0.0
0.2
0.4
0.6
0.8
|p| GeV

Wave function decomposition: $N(1440)$ cf. $\Delta(1600)$

	$N(940)$	$N(1440)$	$\Delta(1232)$	$\Delta(1600)$
scalar	62%	62%	–	–
pseudovector	29%	29%	100%	100%
mixed	9%	9%	–	–
S-wave	0.76	0.85	0.61	0.30
P-wave	0.23	0.14	0.22	0.15
D-wave	0.01	0.01	0.17	0.52
F-wave	–	–	~ 0	0.02

$N(1440)$

- Roper's diquark content are almost identical to the nucleon's one.
- It has an orbital angular momentum composition which is very similar to the one observed in the nucleon.

$\Delta(1600)$

- $\Delta(1600)$'s diquark content are almost identical to the $\Delta(1232)$'s one.
- It shows a dominant $\ell = 2$ angular momentum component with its S-wave term being a factor 2 smaller.

The presence of all angular momentum components compatible with the baryon's total spin and parity is an inescapable consequence of solving a realistic Poincaré-covariant Faddeev equation

Studies of N* photo- and electro-couplings

Transition form factors of nucleon resonances

Unique window into their quark and gluon structure → Distinctive information on the roles played by emergent phenomena in QCD

Broad range of photon virtuality → Probe the excited nucleon structures at perturbative and non-perturbative QCD scales

A vigorous experimental program has been and is still under way worldwide

CLAS, CBELSA, GRAAL, MAMI and LEPS

☞ Multi-GeV polarized cw beam, large acceptance detectors, polarized proton/neutron targets.

☞ Very precise data for 2-body processes in wide kinematics (angle, energy): $\gamma p \to \pi N$, ηN, KY.

☞ More complex reactions needed to access high mass states: $\pi\pi N$, $\pi\eta N$, ωN, ϕN, ...

Extract s-channel resonances

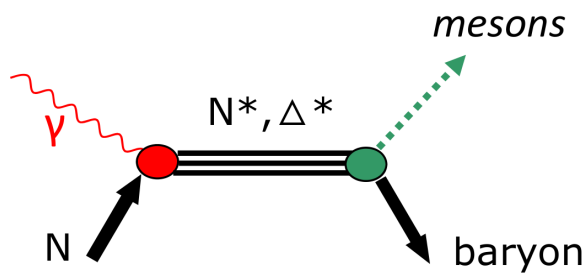

Nucleon Resonance Photo-/Electrocouplings Determined from Analyses of Experimental Data on Exclusive Meson Electroproduction off Protons

Definition (docx) of $A_{1/2}$, $A_{3/2}$ and $S_{1/2}$ electrocouplings
(in pdf format)

Links to the files with electropcoupling values (docx marked by resonance symbols/unmarked pdf)

$\Delta(1232)3/2^+$	$N(1440)1/2^+$	$N(1520)3/2^-$	$N(1535)1/2^-$	$\Delta(1620)1/2^-$	$N(1650)1/2^-$
pdf	pdf	pdf	pdf	pdf	pdf
$N(1675)5/2^-$	$N(1680)5/2^+$	$\Delta(1700)3/2^-$	$N(1710)1/2^+$	$N(1720)3/2^+$	
pdf	pdf	pdf	pdf	pdf	

https://userweb.jlab.org/~mokeev/resonance_electrocouplings/

☞ CLAS12 aims to measure the N^* photo- and electro-couplings at Q^2 ever achieved so far and thus trying to distinguish between different effective degrees of freedom.

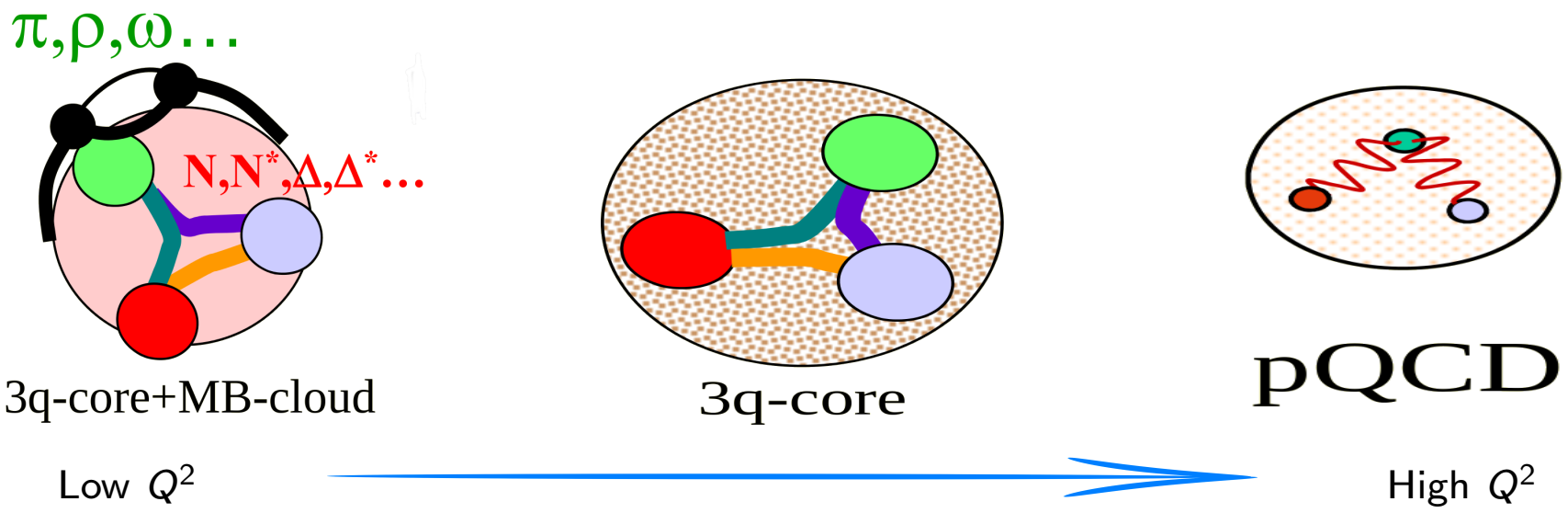

☞ CLAS12 will be able to extract information about fundamental quantities in QCD at an intermediate energy region.

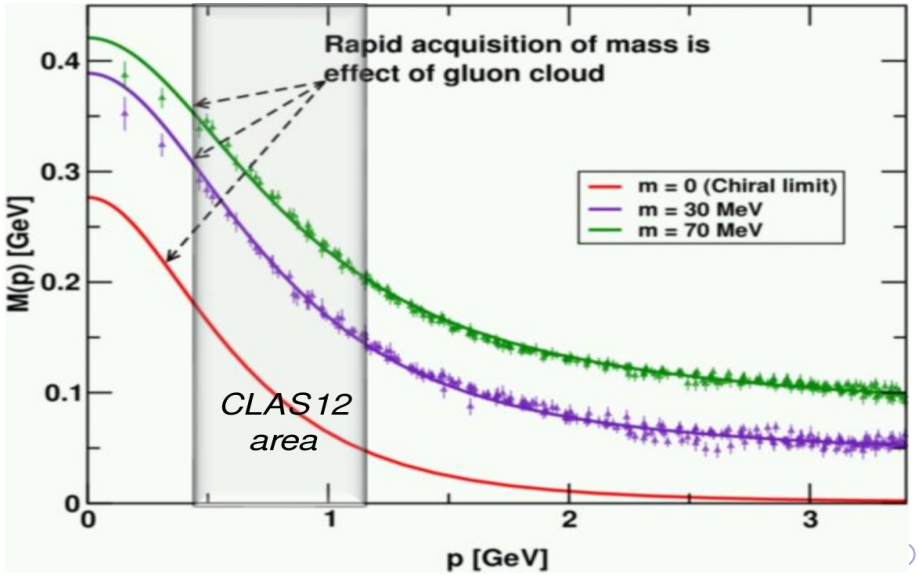

The $\gamma^{(*)}N(940) \to N(940)$ reaction (I)

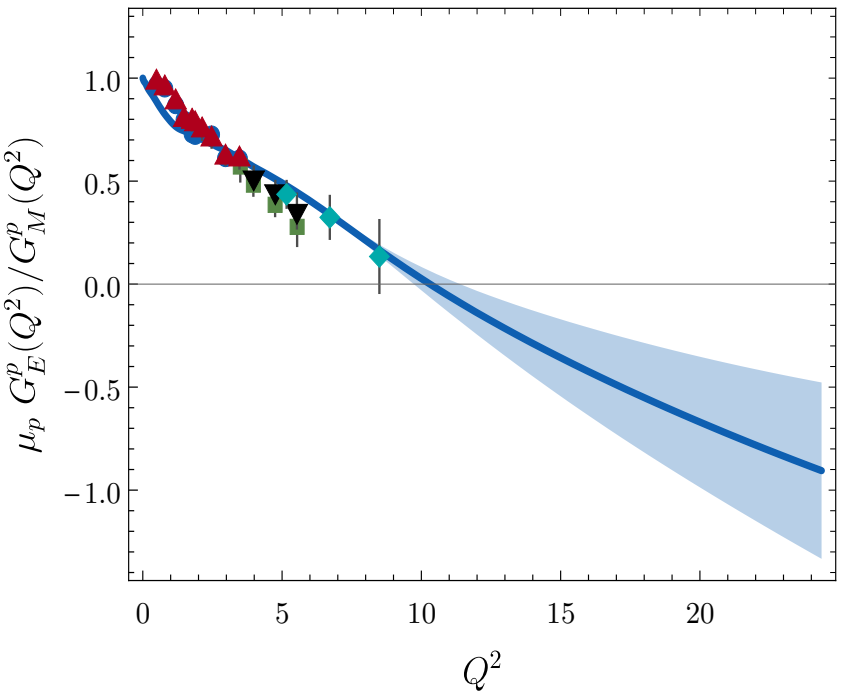

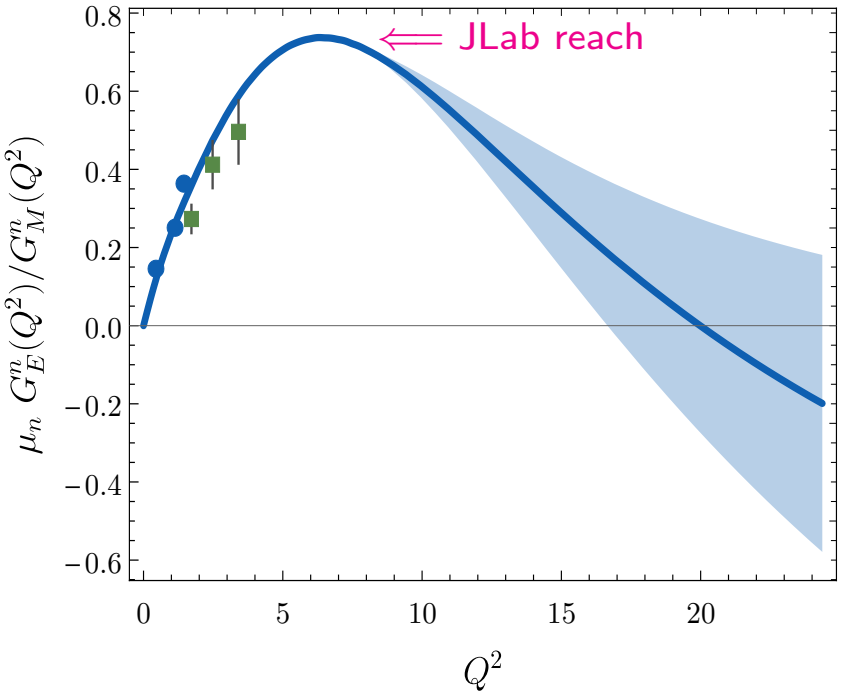

Z.-F. Cui *et al.*, Phys. Rev. D102 (2020) 014043.

☞ Observations:

- There is no evidence for scaling in Dirac and Pauli form factors, and thus in the electromagnetic Sach form factors.
- Our analysis predicts a zero for the proton's electromagnetic ratio at $Q^2 = 10.3^{+1.1}_{-0.7}\,\mathrm{GeV}^2$.
- The neutron's electromagnetic ratio has a peak at $Q^2 \approx 6\,\mathrm{GeV}^2$ and then crosses zero for $Q^2 = 20.1^{+10.6}_{-3.5}\,\mathrm{GeV}^2$.
- All these features can be related with both quark-quark and angular momentum correlations within the nucleon.

The $\gamma^{(*)}N(940) \to N(940)$ reaction (II)

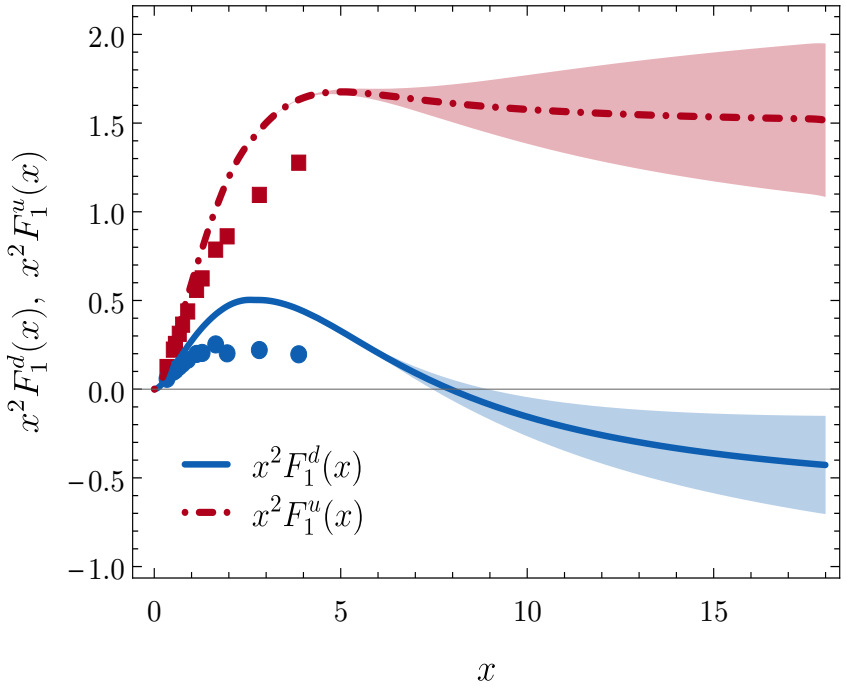

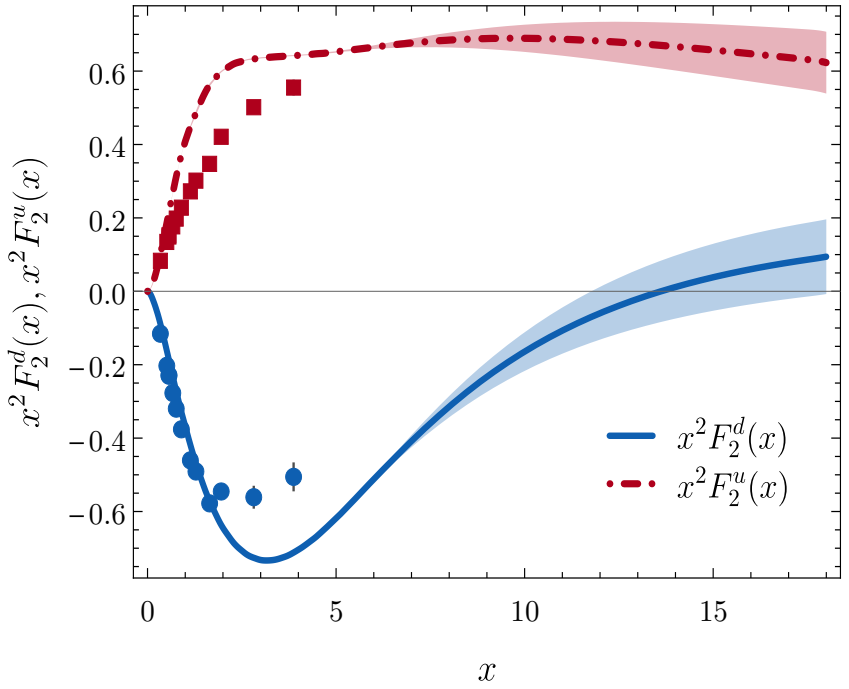

☞ Observations:

- F_1^d is smaller than F_1^u, even allowing for the difference in normalisation, and decreases more quickly as x increases.
- The location of the zero in F_1^d is a measure of the relative probability of finding pseudovector and scalar diquarks in the proton.
- The u- and d-quark Pauli form factors are roughly equal in magnitude on $x \lesssim 5$; *i.e.* F_2^d is suppressed with respect F_2^u but only at large momentum transfer.
- There are contributions playing an important role in F_2, like the anomalous magnetic moment of dressed-quarks or meson-baryon final-state interactions.

The $\gamma^{(*)}N(940) \to N(1440)$ reaction (I)

Nucleon-to-Roper transition form factors at high virtual photon momenta penetrate the meson-cloud and thereby illuminate the dressed-quark core

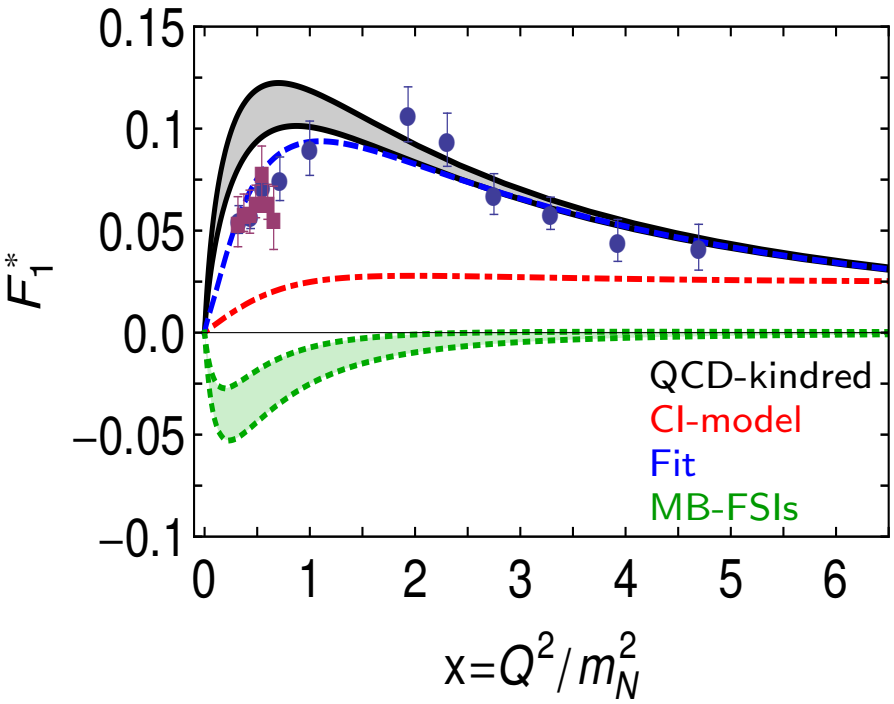

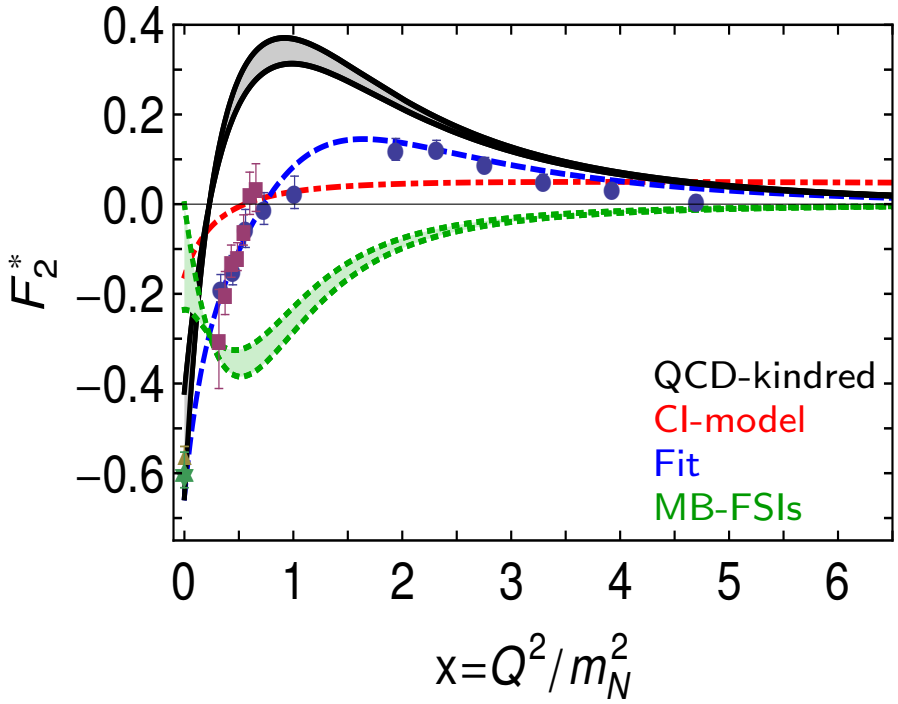

☞ Observations:

- Our calculation agrees quantitatively in magnitude and qualitatively in trend with the data on $x \gtrsim 2$.
- The mismatch between our prediction and the data on $x \lesssim 2$ is due to meson cloud contribution.
- The dotted-green curve is an inferred form of meson cloud contribution from the fit to the data.

CLAS12 detector at JLab will deliver data on the Roper-resonance electroproduction form factors out to $Q^2 \sim 12 m_N^2$ in both the charged and neutral channels

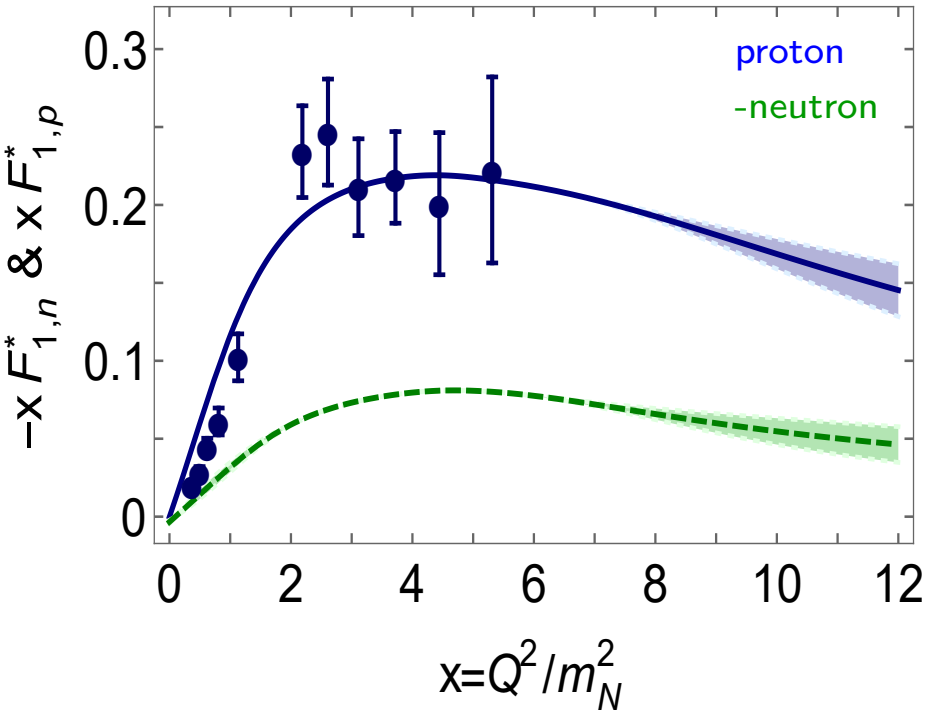

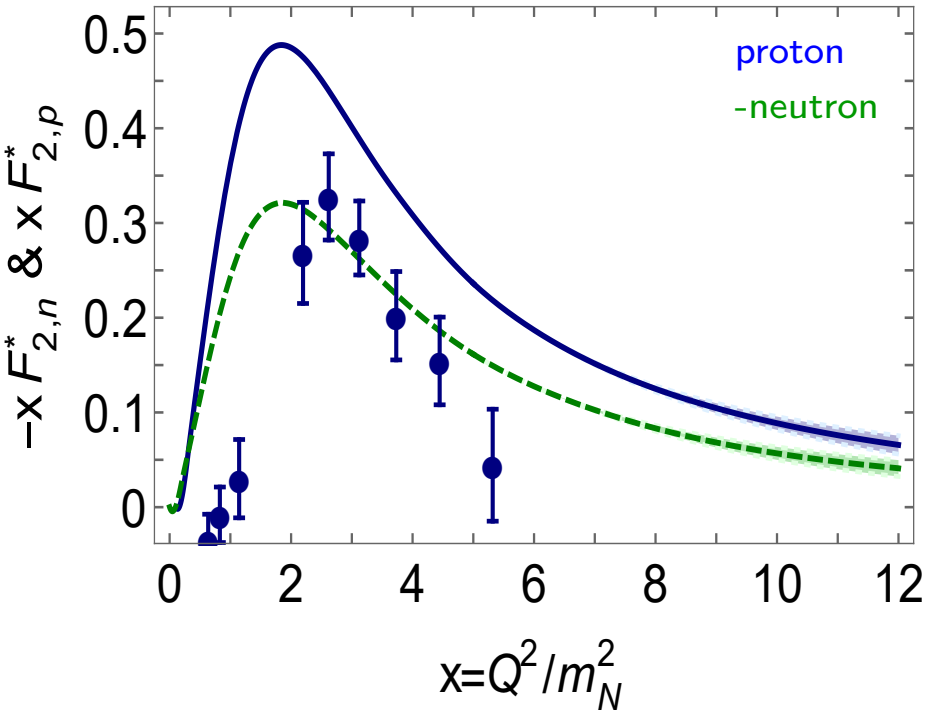

☞ Observations:

- On the domain depicted, there is no indication of the scaling behavior expected of the transition form factors: $F_1^* \sim 1/x^2$, $F_2^* \sim 1/x^3$.
- Since each dressed-quark in the baryons must roughly share the momentum, Q, we expect that such behaviour will only become evident on $x \gtrsim 20$.

Presentations of experimental data typically use the Ash convention

– $G^*_{M,Ash}(Q^2)$ falls faster than a dipole –

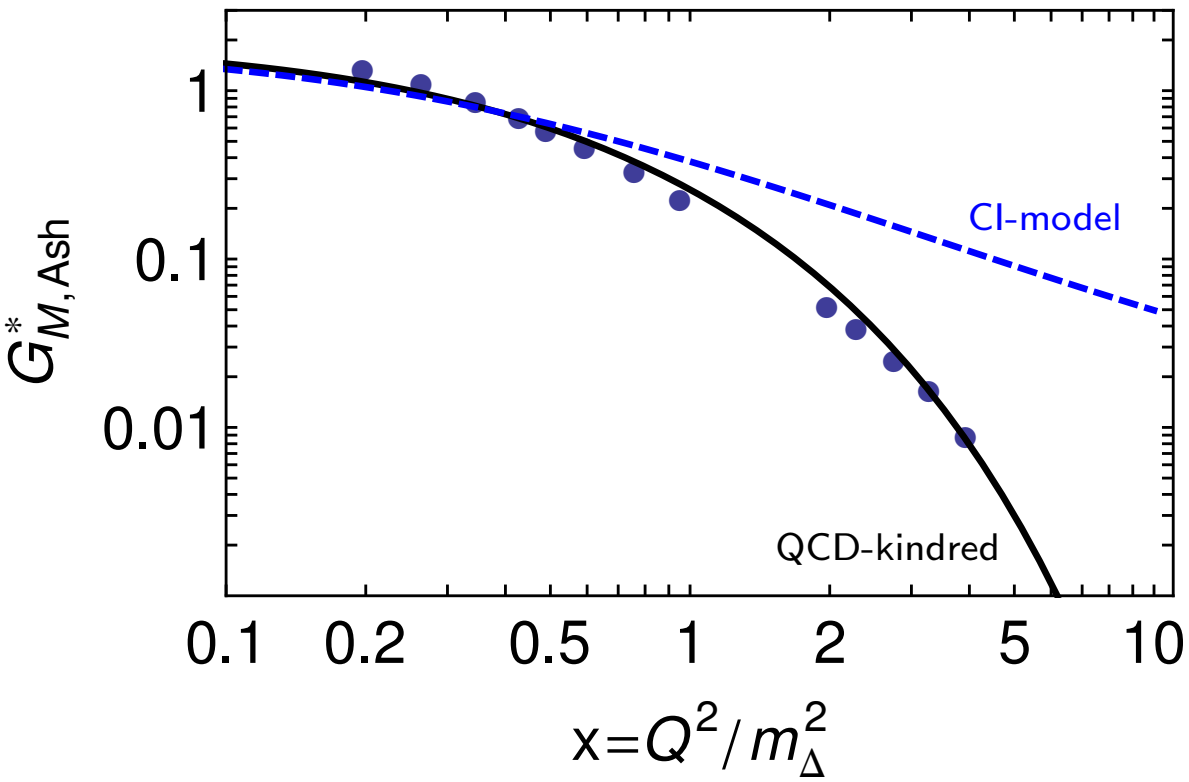

- No sound reason to expect:

  $G^*_{M,\mathrm{Ash}}/G_M \sim$ constant

- Jones-Scadron must exhibit:

  $G^*_{M,\mathrm{J\text{-}S}}/G_M \sim$ constant

- Meson-cloud effects
  - Up-to 35% for $Q^2 \lesssim 2.0 m_\Delta^2$.
  - Soft $\to$ disappear rapidly.

- $G^*_{M,\mathrm{Ash}}$ vs $G^*_{M,\mathrm{J\text{-}S}}$
  - A Difference of $1/\sqrt{Q^2}$.

The $\gamma^{(*)}N(940) \to \Delta(1232)$ reaction (II)

☞ $R_{EM} = R_{SM} = 0$ in SU(6)-symmetric CQM.

- Deformation of the hadrons involved.
- Modification of the transition current.

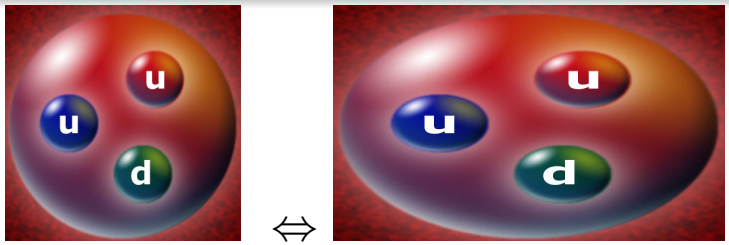

☞ R_{SM}: Good description of the rapid fall at large momentum transfer.

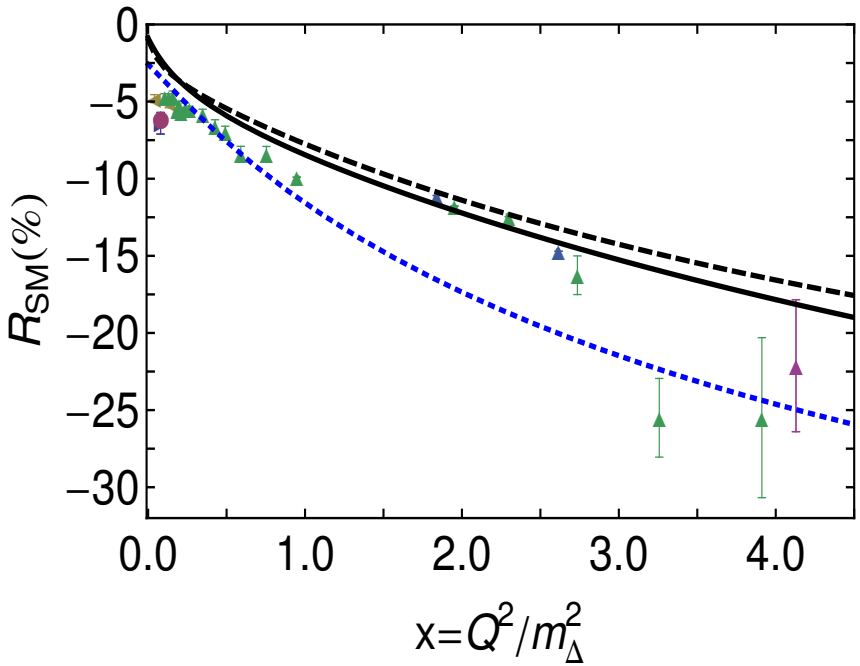

☞ R_{EM}: A particularly sensitive measure of orbital angular momentum correlations.

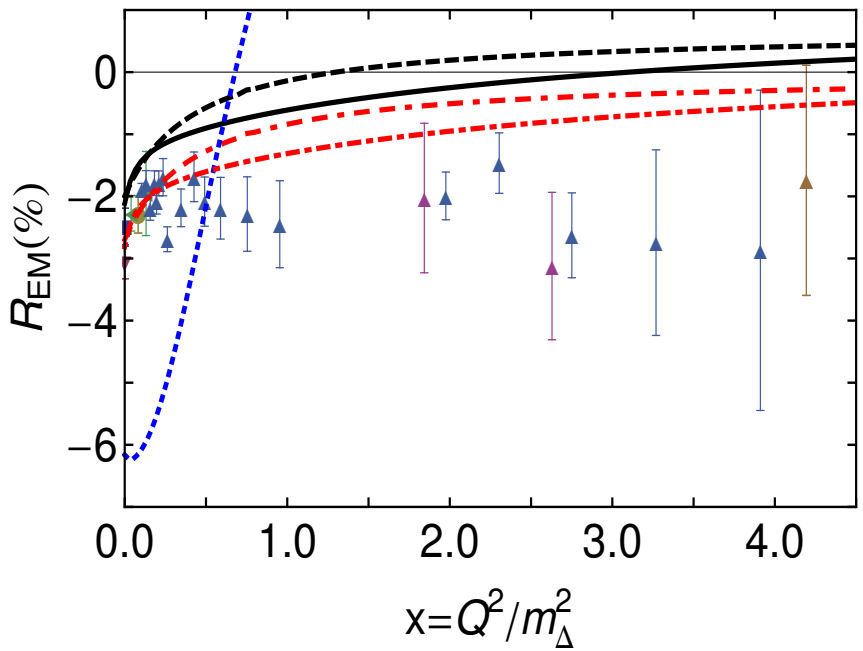

☞ *Zero Crossing in the electric transition form factor:*

$$\textit{Contact interaction} \to Q^2 \sim 0.75 m_\Delta^2 \sim 1.14\ GeV^2$$

$$\textit{QCD-kindred interaction} \to Q^2 \sim 3.25 m_\Delta^2 \sim 4.93\ GeV^2$$

Large Q^2-behavior of the quadrupole ratios

Helicity conservation arguments in pQCD should apply equally to:

- *Results obtained within our QCD-kindred framework;*
- *Results produced by a symmetry-preserving treatment of a contact interaction.*

$$R_{EM} \overset{Q^2\to\infty}{=} 1\,, \quad R_{SM} \overset{Q^2\to\infty}{=} \textit{constant}\,.$$

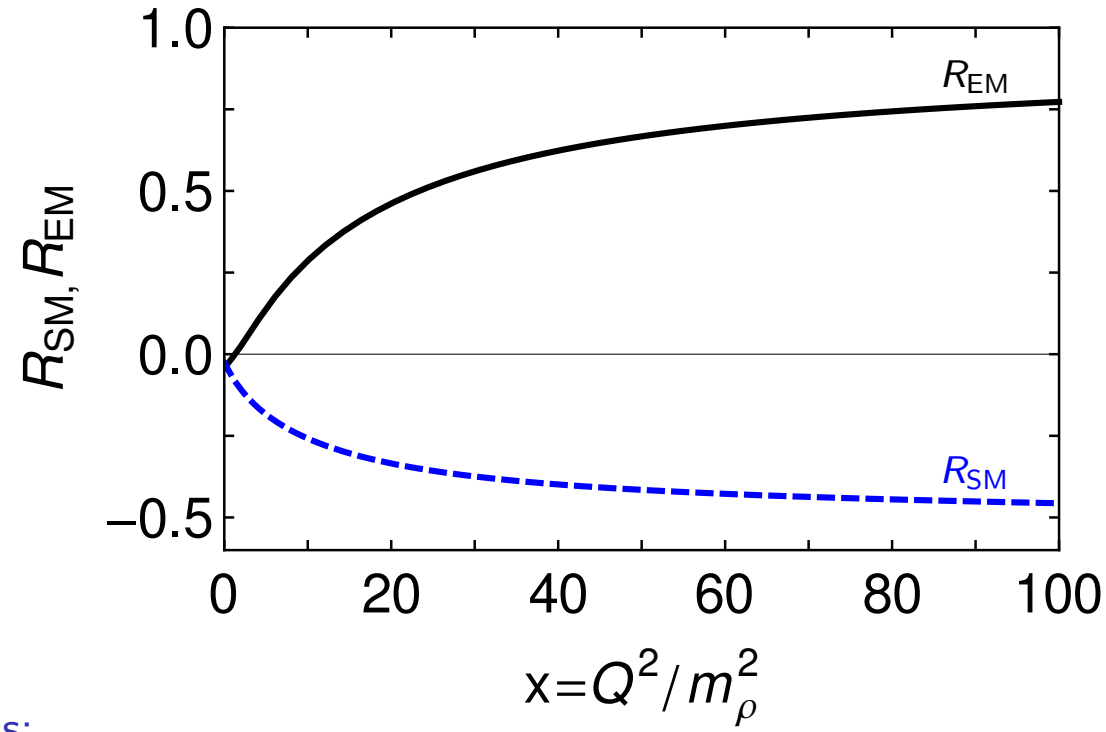

☞ Observations:

- Truly asymptotic Q^2 is required before predictions are realized.
- $R_{EM} = 0$ at an empirical accessible momentum and then $R_{EM} \to 1$.
- $R_{SM} \to$ constant. Curve contains the logarithmic corrections expected in QCD.

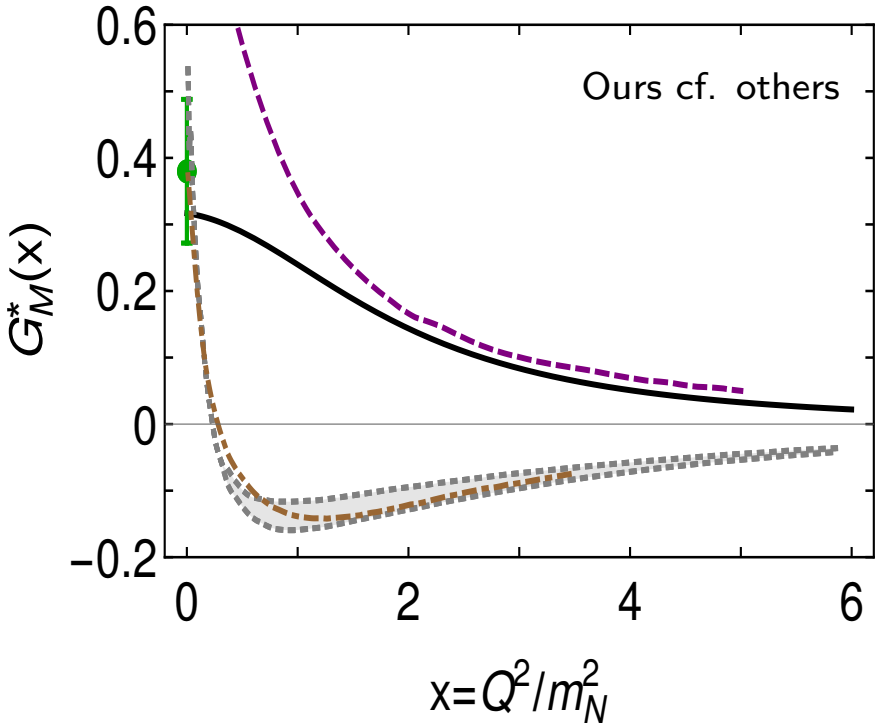

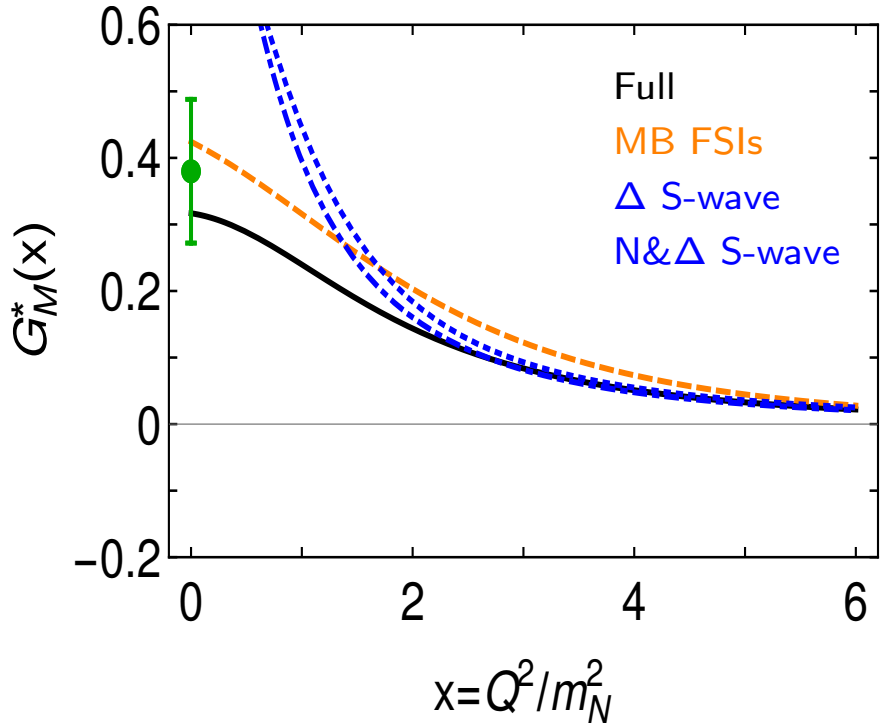

☞ Observations:

- It is positive defined in the whole range of photon momentum and decreases smoothly with larger Q^2-values.
- The mismatch with the empirical result are comparable with that in the $\Delta(1232)$ case, suggesting that MB FSIs are of similar importance in both channels.
- Higher partial-waves have a visible impact on G_M^*: They bring the magnetic dipole moment to lower values which could be compatible with experiment.

The $\gamma^{(*)}N(940) \to \Delta(1600)$ reaction (II)

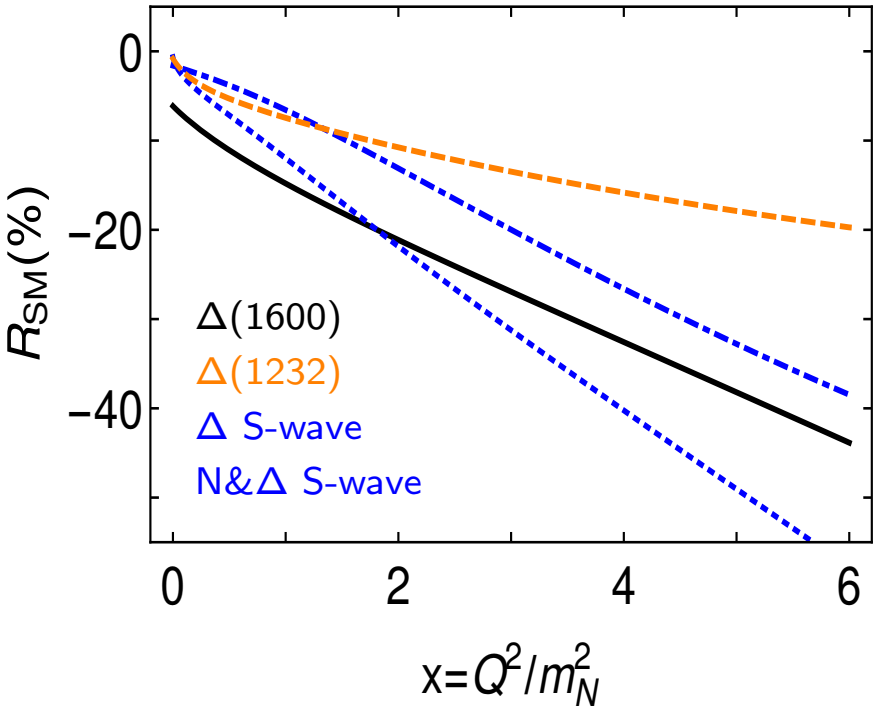

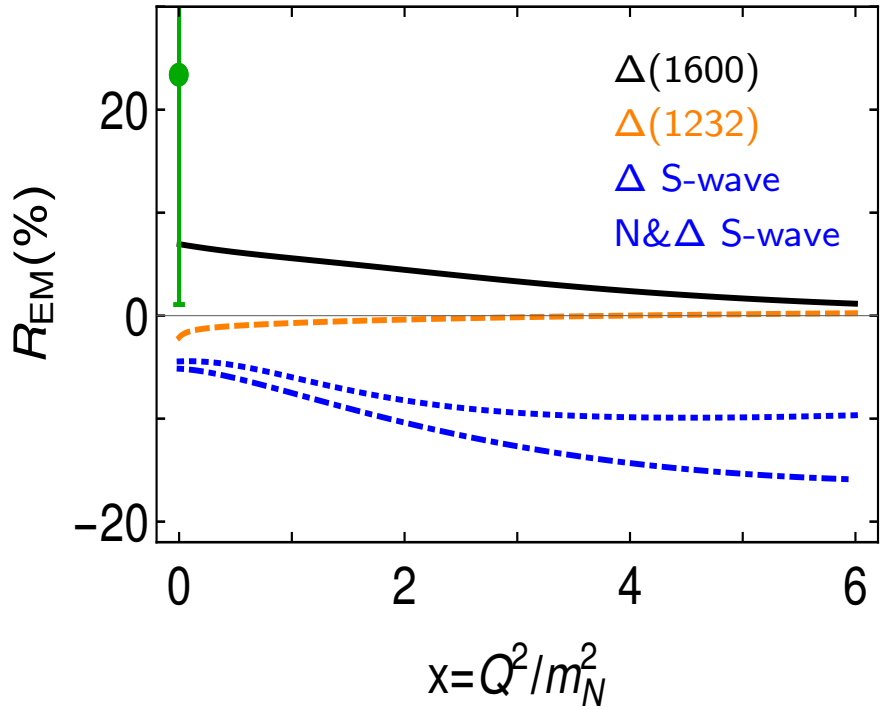

☞ Observations:

- $R_{SM}^{\Delta'} \gtrsim R_{SM}^{\Delta}$ indicating that higher orbital angular momentum components in the $\Delta(1600)$ are more important than in the $\Delta(1232)$.
- R_{EM} for the $\Delta(1600)$ transition is far larger in magnitude than the analogous result for the $\Delta(1232)$ (and opposite in sign).
- Points above are an observable manifestation of important higher orbital angular momentum components in both states.
- In particular, there is an enhanced D-wave strength in the $\Delta(1600)$ relative to that in the $\Delta(1232)$.

Summary and conclusions (I)

We insist on our purpose of getting an unified study of EM elastic and transition form factors of nucleon resonances using QCD-kindred kernels and interaction vertices

☞ **The $\gamma^*\mathrm{N} \to \mathrm{Nucleon}\,[\equiv \mathrm{N}(940)]$ reaction:**

- Proton's and neutron's electromagnetic ratios are sensible observables to disentangle fundamental quantities of QCD.
- The presence of strong diquark correlations within the nucleon is sufficient to understand empirical extractions of the flavor-separated form factors.
- Scalar diquark dominance and the presence of higher orbital angular momentum components are responsible of the Q^2-behaviour of G_E^p/G_M^p and F_2^p/F_1^p.

☞ **The $\gamma^*\mathrm{N} \to \mathrm{Nucleon}'\,[\equiv \mathrm{N}(1440)]$ reaction:**

- The Roper is the proton's first radial excitation. It consists on a dressed-quark core augmented by a meson cloud that reduces its mass by approximately 20%.
- Our calculation agrees quantitatively in magnitude and qualitatively in trend with the data on $x \gtrsim 2$. The mismatch on $x \lesssim 2$ is due to meson-cloud contribution.
- CLAS12@JLab will test our predictions for the charged and neutral channels in a range of momentum transfer larger than $4.5\,\mathrm{GeV}^2$.

Summary and conclusions (II)

☞ **The $\gamma^* \mathrm{N} \to \mathrm{Delta}\,[\equiv \Delta(1232)]$ reaction:**

- $G^{*p}_{M,J-S}$ falls asymptotically at the same rate as G^p_M. This is compatible with isospin symmetry and pQCD predictions.
- Data do not fall unexpectedly rapid once the kinematic relation between Jones-Scadron and Ash conventions is properly account for.
- Limits of pQCD, $R_{EM} \to 1$ and $R_{SM} \to$ constant, are apparent in our calculation but truly asymptotic Q^2 is required before the predictions are realized.

☞ **The $\gamma^* \mathrm{N} \to \mathrm{Delta}'\,[\equiv \Delta(1600)]$ reaction:**

- G^*_M and R_{EM} are consistent with the empirical values at the real photon point, but we expect inclusion of MB FSIs to improve the agreement on $Q^2 \sim 0$
- R_{EM} is markedly different for $\Delta(1600)$ than for $\Delta(1232)$, highlighting the sensitivity of G^*_E to the degree of deformation of the Δ-baryons.
- R_{SM} is qualitatively similar for both $\gamma^* N \to \Delta(1600)$ and $\gamma^* N \to \Delta(1232)$ transitions, still larger (in absolute value) for the $\Delta(1600)$ case.